RSC Advances

ROYAL SOCIETY
OF CHEMISTRY

www.rsc.org/advances

Journal Name

RSCPublishing

ARTICLE

Cite this: DOI: 10.1039/x0xx00000x

Fabrication of Host–Guest UV-Blocking Materials by Intercalation of Fluorescent Anions into Layered Double Hydroxides

Guirong Wang,[a] Simin Xu,[a] Chunhui Xia,[a] Dongpeng Yan,*[,a,b] Yanjun Lin,*[,a] and Min Wei[a]

Received 00th January 2012, Accepted 00th January 2012

DOI: 10.1039/x0xx00000x

www.rsc.org/

Materials for blocking UV light play important roles in a variety of areas such as protecting the human skin and increasing the lifetime of polymers. In this work, a new type of host–guest UV-blocking material has been synthesized by the introduction of a fluorescent anion, 2-[2-[4-[2-(4- carboxyphenyl)vinyl]phenyl]vinyl]benzoate (CPBA), into the interlayer galleries of a ZnAl–NO_3 layered double hydroxide (LDH) precursor by an anion-exchange method. The structure and the thermal and photostability of the intercalated ZnAl–CPBA-LDH were investigated by powder X-ray diffraction (XRD), infrared spectroscopy (FTIR), thermogravimetry and differential thermal analysis (TG–DTA), fluorescence spectroscopy and UV–vis spectroscopy. The supramolecular layered host–guest structure of ZnAl–CPBA-LDH enables both physical shielding and absorption of UV light. Furthermore, in contrast to conventional UV blocking materials—which convert UV light into thermal energy—the CPBA anions in the LDH interlayer galleries convert UV light (in the range 250–380 nm) into lower energy fluorescence emission ($\lambda_{\max}^{\mathrm{em}}$ = 430 nm), thus reducing the thermal aging of the polymer composite materials. Intercalation of the CPBA anions into the LDH host also markedly enhances the thermal stability of CPBA. In polypropylene (PP) aging performance tests, after adding 1 wt.% –5 wt.% ZnAl–CPBA-LDH to PP, the resistance to UV degradation of the resulting ZnAl–CPBA-LDH/PP composites is higher than that of pristine PP or a CPBA/PP composite. Therefore, this work provides a way to construct a new type of host–guest layered materials for UV-blocking applications.

Introduction

UV light radiation can produce highly reactive free radicals that can induce chemical reactions, resulting in subsequent photodegradation[1], and color fading of polymers[2], pigments, and dyes, a process which is usually called aging. In addition to UV light aging, polymers also suffer from thermal aging, with both types of aging causing loss of mechanical strength of the polymers.[3]

The development of additives able to protect materials against UV light aging has therefore attracted significant interest.[4] UV blocking materials can be classified into two types—inorganic UV shielding materials and organic UV absorbing materials—on the basis of the blocking mechanism involved. A small number of inorganic shielding materials, such as titanium dioxide and zinc oxide, protect the skin or polymer materials by reflecting and scattering UV radiation. A wider variety of organic UV absorbing materials have been employed, including camphors, benzophenones, cinnamates, and triazines. However, organic UV absorbing materials have poor thermal and photostability which reduces their long-term efficacy as additives in polymers, and the radical species produced by decomposition of the organic UV absorbing material can even contribute to an enhanced rate of degradation of the polymer.[5] Furthermore the UV energy absorbed by the organic material is generally dissipated as heat, which promotes the thermal aging of polymer materials to a certain extent. Incorporating organic UV absorbing materials in an inorganic host matrix offers several potential advantages. The resulting hybrid absorber can block UV light by both physical screening by virtue of the inorganic host and absorption by the organic guest. Furthermore incorporating an organic absorber in an inorganic host should increase its thermal and photostability when used as an additive in polymers. Host–guest materials also have potential advantages as sunscreen agents, since organic UV absorbing molecules pose problems in terms of both environmental pollution and health and safety,[6] and incorporating them in an inorganic host will decrease their direct contact with the skin.

Layered double hydroxides (LDHs) are one such potential inorganic host matrix. LDHs are a class of anionic clays[7] which have received much attention from both the chemical industry and academia in view of their actual and potential applications in catalysis,[8] electrode materials[9] and polymer additives[10]. Recently, simple LDHs containing inorganic anions have been employed as inorganic UV blocking materials for the protection of asphalt and rubber against UV aging.[7b, 11] Furthermore, the LDH layers can enhance the oxygen barrier properties of a polymer[12] and absorb the reactive free radicals produced during the polymer aging process.[13] This can inhibit both the UV aging and thermal aging processes, since free radicals and oxygen are usually the main factors affecting these aging processes.

Many kinds of organic anions can be intercalated into the interlayer galleries of LDHs to form functional materials with a supramolecular layered structure. In this work, we focus on the intercalation of a fluorescent guest anion. In addition to the benefits afforded by the host–guest structure discussed above, a fluorescent guest offers additional advantages in its own right. In contrast to conventional UV blocking materials—which convert UV light into thermal energy—fluorescent anions absorb high energy UV light (in the range 250–380 nm) and convert it into lower energy fluorescence emission in the visible region, thus reducing the thermal aging of the polymer composite materials. In addition, if the fluorescence emission is in the blue region of the visible spectrum, the material can act as a fluorescent whitening agent (FAW) or optical brightener and counteract the yellow appearance of many polymer products in natural light. 2-[2-[4-[2-(4-cyanophenyl)vinyl]phenyl]vinyl]benzonitrile (CPB, Scheme 1A) is an example of FAW, which can serve as UV absorber towards UV-blocking applications, and has been widely used in the paper and textile industries. Moreover, the phenylenevinylene group in CPB molecule is a typical chromophore, which can transfer UV light into fluorescence emission effectively. As a neutral molecule, CPB cannot be directly intercalated into an LDH host, but simple hydrolysis to its carboxylic acid analogue (Scheme 1B) allows the carboxylate anions CPBA to be intercalated into the interlayer galleries of a ZnAl-LDH host to afford ZnAl–CPBA-LDH (Scheme 1C). The product was characterized by a range of physicochemical methods and was also added to PP to assess its UV blocking properties and antiaging performance.

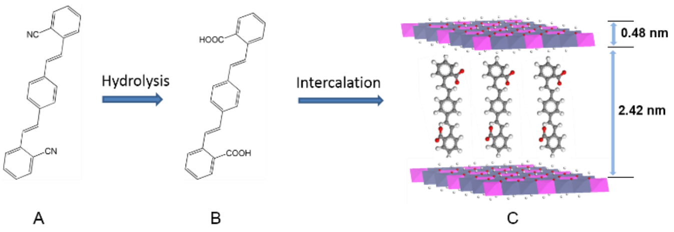

Scheme 1. Chemical structure and schematic representation of (A) CPB, (B) CPBA, (C) ZnAl–CPBA-LDH and the hydrolysis and intercalation process.

Experimental section

2.1. Reagents.

Analytical grade $Zn(NO_3)_3$ $6H_2O$, $Al(NO_3)_3$ $9H_2O$, NaOH, H_2SO_4 and CPB were purchased from Beijing Chemical Co., Ltd. and used without further purification. CO_2-free deionized water was used in synthesis and washing steps. Commercial isotactic polypropylene (PP, S1003) was purchased from Yanshan Petrochemical Company, China.

2.2. Preparation of ZnAl–NO_3-LDH.

The ZnAl–NO_3-LDH precursor was prepared by the method involving separate nucleation and aging steps (SNAS) developed in our laboratory.[14] A solution of $Zn(NO_3)_2$ $6H_2O$ and $Al(NO_3)_3$ $9H_2O$ with a Zn/Al ratio of 2.0 in CO_2-free deionized water ($[Zn^{2+}] + [Al^{3+}] = 0.9$ M) and a solution of NaOH (1.8 M) in CO_2-free deionized water were simultaneously added to a modified colloid mill with a rotor speed of 3000 rpm and mixed for 1 min. The resulting suspension was removed from the colloid mill as soon as possible and aged at 100 ℃ for 6 h under N_2 protection. The final suspension was washed several times with CO_2-free deionized water until the pH of the washings was around 7, separated by centrifugation, and finally dried at 60 ℃ for 24 h.

2.3. Preparation of CPBA and ZnAl–CPBA-LDH.

CPB was hydrolyzed to give CPBA by heating at 130 ℃ with 50 wt.% H_2SO_4 as a catalyst. CPBA anion intercalated LDH (ZnAl–CPBA-LDH) was prepared by anion-exchange using ZnAl–NO_3-LDH as a precursor. ZnAl–NO_3-LDH (0.018 mol) was sufficiently dispersed in CO_2-free deionized water to form a slurry. CPBA (0.03 mol) was dissolved in CO_2-free deionized water to form an aqueous solution. The pH value of the CPBA aqueous solution was adjusted to around 8 by adding NaOH aqueous solution and it was then directly mixed with the precursor slurry, followed by aging at refluxing temperature for 6 h under N_2 protection. The resulting precipitate was centrifuged, thoroughly washed (using CO_2-free deionized water and finally anhydrous ethanol), and dried at 70 ℃ overnight.

2.4. Preparation of ZnAl–CPBA-LDH/PP, CPBA/PP, ZnAl–NO_3-LDH/PP and pristine PP Films.

0.5 g of ZnAl–CPBA-LDH, 0.5 g of CPBA, 0.5 g of ZnAl–NO_3-LDH (1 wt.%), 1.5 g of ZnAl–NO_3-LDH (3 wt.%), and 2.5 g of ZnAl–NO_3-LDH (5 wt.%) were mixed with separate portions of 50.0 g of PP in a Haake internal mixer (HAAKE Rheomix 600 OS, Thermo Fisher Scientific, America) equipped with two counter-rotating rotors at 185 ℃ for about 10 min to produce the corresponding composites. The resulting composites were molded into flakes of 100 mm × 100 mm × 1 mm, and films with 0.05 mm thickness at 180 ℃ under pressure. Pristine PP films were also prepared under the same conditions as a reference.

2.5. Photostability of CPBA/PP, ZnAl–CPBA-LDH/PP, ZnAl–NO_3-LDH/PP and pristine PP Films.

Samples of ZnAl–CPBA-LDH/PP, CPBA/PP, ZnAl–NO_3-LDH/PP and pristine PP films were rapidly photo-aged in a UV photo-aging instrument (with a UV high-pressure mercury lamp as the UV light source, a power of 1000 W and $\lambda_{max} = 365$ nm) with a temperature-control system holding the temperature at 60 ℃. FTIR spectra were recorded after irradiation for 10 min. The process was repeated five times, giving a total of 50 min of accumulated exposure for each sample.

2.6. Characterization of samples.

Powder X-ray diffraction (PXRD) patterns were recorded on a Rigaku XRD-6000 diffractometer, using Cu Kα radiation ($\lambda = 0.15418$ nm) at 40 kV, 30 mA, with a scanning rate of 5 °/min, in the 2θ range from 2 ° to 70 °. FTIR spectra were recorded on a Bruker Vector 22 Fourier transfer infrared spectrophotometer using the KBr disk method with a ratio of sample/KBr of 1:100 by mass. Thermogravimetric (TG) analysis was performed on a Beifen PCT-IA instrument in the temperature range 25–700 ℃ with a heating rate of 10 ℃ min^{-1} in air. Scanning electron microscopy (SEM) images were obtained using a Hitachi S-4700 scanning electron microscope operating at 20 kV. Transmission electron microscopy (TEM) and high resolution TEM (HRTEM) observations were carried out on a JEOL JEM-2100 transmission electron microscope. Diffuse reflectance UV spectra were recorded with a PerkinElmer Lamda 950 fitted with a $BaSO_4$ integrating sphere. The fluorescence spectra were recorded on a RF-5301PC spectrofluorophotometer with an excitation wavelength of 350 nm. The fluorescence emission spectra were recorded in the range 400–650 nm, and both the excitation and emission slit were set to 3 nm. UV-irradiated samples were analyzed immediately after exposure.

Results and Discussion

3.1. X-ray Diffraction

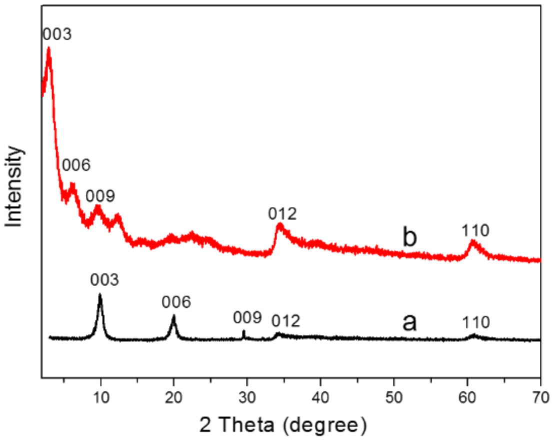

Figure 1. XRD patterns of (a) ZnAl–NO_3-LDH and (b) ZnAl–CPBA-LDH.

The XRD patterns of ZnAl–NO_3-LDH and ZnAl–CPBA-LDH are shown in Figure 1. The XRD pattern of the ZnAl–NO_3-LDH precursor (Figure 1a) exhibits the typical characteristics of an LDH phase. The (003), (006), and (009) diffraction peaks, which correspond to the basal and higher order reflections, appear at 9.66°, 19.56°, and 29.36°, respectively. The interlayer distance d_{003} is 0.90 nm, which is close to the value reported in the literature.[15] After CPBA anions were intercalated into the interlayer galleries of ZnAl–NO_3-LDH, the main characteristic reflections of the product appear at 2.99° (003), 6.05° (006), 9.83° (009), and 60.68° (110) and the d_{003} (2.903 nm), d_{006} (1.445 nm) and d_{009} (0.925 nm) spacings present a good multiple relationship for the basal, second and third-order reflections (Figure 1b). The lattice parameter *c* can be calculated from averaging the positions of the three harmonics: $c = 1/3\ (d_{003} + 2\ d_{006} + 3\ d_{009})$. The basal spacing for ZnAl–CPBA-LDH is 2.903 nm, indicating that CPBA anions have replaced NO_3^- in the interlayer galleries. Considering the thickness of the LDH layer (0.48 nm), the spacing of the gallery between the LDH layers is about 2.42 nm, which corresponds to a single layer of CPB anions being intercalated perpendicular to the LDH layers.

3.2. FT-IR spectroscopy

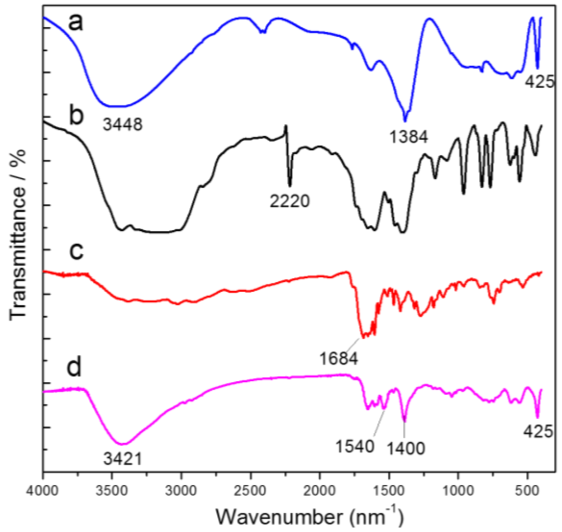

Figure 2. FT-IR spectra of (a) ZnAl–NO_3-LDH, (b) CPB, (c) CPBA, and (d) ZnAl–CPBA-LDH

The FT-IR spectra of ZnAl–NO_3-LDH, CPB, CPBA and ZnAl–CPBA-LDH are shown in Figure 2. The broad absorption band around 3448 cm^{-1} shown in the spectrum of the ZnAl–NO_3-LDH precursor (Figure 2a) can be ascribed to the stretching vibration of the O–H groups of LDH layers and the interlayer water molecules[16]. The sharp band around 1384 cm^{-1} corresponds to the υ_3 stretching vibration of NO_3^- groups and the band at 425 cm^{-1} can be ascribed to O–M–O vibrations in the layers of LDH.[17] Figure 2b shows a sharp absorption peak at 2220 cm^{-1} which can be assigned the stretching vibration of the C≡N groups in the CPB. In Figure 2c, the absorption peak at 2220 cm^{-1} has disappeared and a peak at 1684 cm^{-1} which can be assigned to the C=O stretching vibration of the carboxylic acid group is present, indicating the successful hydrolysis of CPB into CPBA. In the spectrum of the ZnAl–CPBA-LDH obtained after intercalation (Figure 2d), the O–H absorption band around 3421 cm^{-1} and the O–M–O vibration band at 425 cm^{-1} are similar to the corresponding bands in the spectrum of the ZnAl–NO_3-LDH precursor, while the characteristic peak of the nitrate group was absent, confirming that the nitrate ions have been displaced by the CPBA anions. The stretching vibration of the carboxylic acid group moved from 1684 cm^{-1} to 1540 cm^{-1} and 1400 cm^{-1} (the antisymmetric and symmetric stretching bands) of the carboxylic group (Figure 2d), suggesting that the carboxylic acid group has been deprotonated to form an anion and has hydrogen bonding interactions with the LDH layers. These results are in agreement with those observed by XRD, further confirming the successful intercalation of the CPBA anions into the interlayer of galleries of ZnAl–NO_3-LDH to form ZnAl–CPBA-LDH.

3.3. TG–DTA Analysis

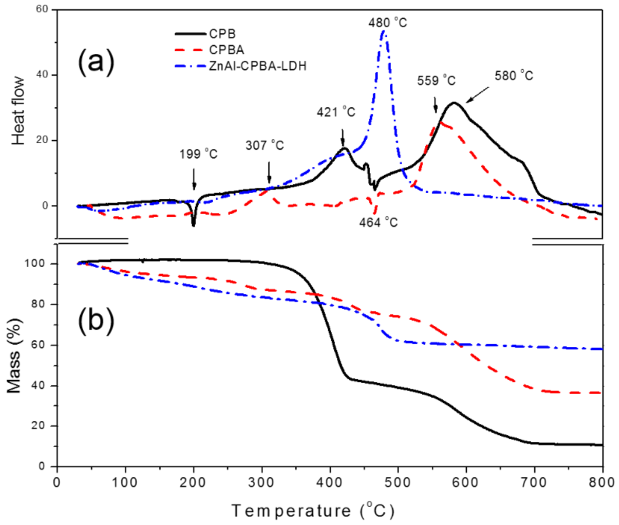

Figure 3. TG (a) and DTA (b) curves of CPB (solid line), CPBA (dashed line), and ZnAl–CPBA-LDH (dot-dashed line).

Figure 3 shows the TG–DTA curves of CPB, CPBA, and ZnAl–CPBA-LDH. For CPB, the endothermic peak at 199 ℃ in the DTA curve correspond to the removal of adsorbed water and the partial decomposition, and the two strong exothermic peaks around 421 ℃ and 580 ℃ separately correspond to the further decomposition and complete combustion of CPB. After CPB was hydrolyzed into CPBA, the first exothermic peak occurred around 307 ℃, and further decomposition and complete combustion followed around 464 ℃ and 559 ℃, respectively, indicating CPBA has better thermal stability than CPB. The DTA curve for ZnAl–CPBA-LDH is quite different from those of CPB and CPBA. The first and second endothermic peaks marked at 125 ℃ and 307 ℃ in the DTA curve correspond to the removal of interlayer water and dehydroxylation, respectively. The DTA curve of ZnAl–CPBA-LDH has a strong exothermic band at 480 ℃ with a corresponding mass loss between 400 ℃ and 600 ℃ in the TG curve which is due to the combustion of the organic guest. The decomposition temperature of the CPBA occurs at 480 ℃, suggesting that the intercalation of the CPBA anions into the interlayer galleries of the ZnAl–NO_3-LDH markedly enhances the thermal stability of the organic guest. This improvement in thermal stability can be ascribed to the interactions between the host brucite-like sheets and the intercalated guest anions, involving electrostatic attraction between opposite charges, hydrogen bonding, and van der Waals forces.

3.4. SEM and TEM

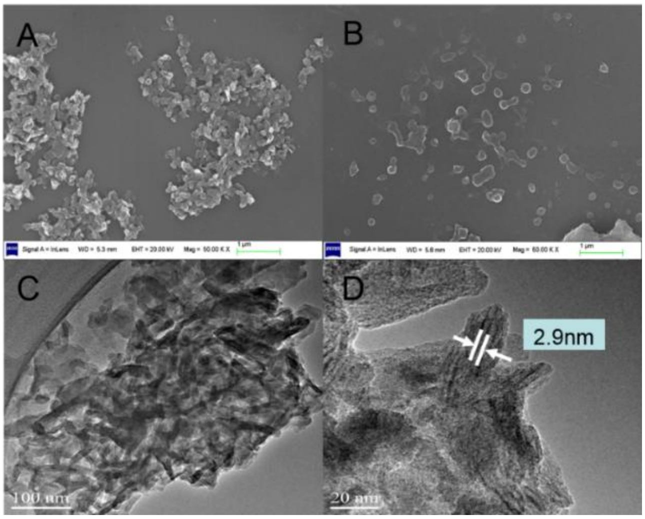

Figure 4. SEM of (A) ZnAl–NO_3-LDH and (B) ZnAl–CPBA-LDH; (C) TEM of ZnAl–CPBA-LDH; (D) HRTEM of ZnAl–CPBA-LDH.

The surface morphology and particle size of ZnAl–NO_3-LDH and ZnAl–CPBA-LDH were investigated by SEM and TEM, as illustrated in Figure 4. The expected hexagonal plate-like nature of the crystallites is clearly apparent in the micrographs of both ZnAl–NO_3-LDH and ZnAl–CPBA-LDH, indicating that the intercalation of CPBA does not change the morphology of the LDH crystallites, as shown by comparison of Figure 4A and Figure 4B. The diameter of the ZnAl–NO_3-LDH platelets is in the range 60–100 nm, while that of ZnAl–CPBA-LDH is in the range 100–150 nm; the increase in particle size after intercalation can be attributed to the ion-exchange reaction being carried out at high temperature. The TEM (Figure 4C) and HRTEM micrographs of ZnAl–CPBA-LDH (Figure 4D) show that the interlayer spacing increased to 2.9 nm after intercalation, which is in accordance with the XRD results.

3.5. UV Absorption Properties of ZnAl–CPBA-LDH.

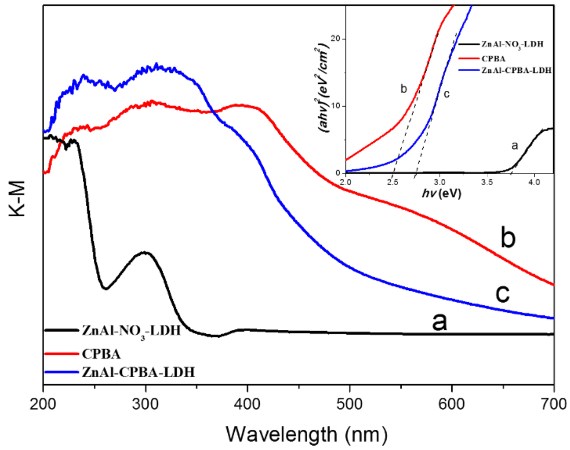

Figure 5. UV–vis diffuse reflectance spectra and absorption threshold of (a) ZnAl–NO_3-LDH, (b) CPBA and (c) ZnAl–CPBA-LDH.

The UV–vis diffuse reflectance spectra of ZnAl–NO_3-LDH, CPBA and ZnAl–CPBA-LDH are shown in Figure 5. The spectrum of ZnAl–NO_3-LDH (Figure 5a) shows strong UV absorption between 200 and 320 nm due to the presence of nitrate anions in the interlayer galleries, as well as the shielding effect of the LDH layers. The UV absorbance curve of CPBA, as shown in Figure 5b, indicates that CPBA has a broad UV absorption between 200 and 500 nm. After intercalation, ZnAl–CPBA-LDH exhibits excellent UV absorption ability below 400 nm, even better than pure CPBA, which is due to the interactions between the guest and host layers.

3.6. Fluorescence properties

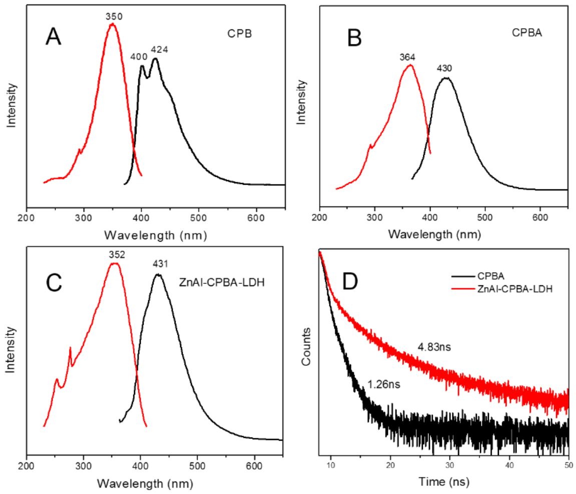

Figure 6. Fluorescence spectra of (A) CPB, (B) CPBA, (C) ZnAl–CPBA-LDH and (D) fluorescence lifetime.

The fluorescence spectra of CPB, CPBA and ZnAl–CPBA-LDH are shown in Figure 7. The excitation spectrum and emission spectrum of CPBA both show a red shift when compared with CPB, due to the C≡N groups in the CPB molecule being hydrolyzed into COOH groups. After intercalation, the emission spectrum of ZnAl–CPBA-LDH remains unchanged with the maximum emission wavelength (λ_{max}^{em}) located at 430 nm, while the excitation spectrum shows a slight blue shift from 364 nm to 352 nm, which can be attributed to intermolecular interactions between the excited guest and the LDH layers.[18] The fluorescence lifetime of ZnAl–CPBA-LDH is 4.83 ns, significantly longer than the value of 1.26 ns for pristine CPBA; the photoluminescence quantum yield (PLQY) of ZnAl–CPBA-LDH increases to 35.4%, compared with a value of 15.6% for pristine CPBA. The improvement of the fluorescence lifetime and PLQY can be assigned to the high degree of organization of the CPBA moieties in the interlayer galleries of the LDH layers, which suppresses the thermal vibration and rotation of the CPBA anions.[19]

3.7. Photostability of ZnAl–CPBA-LDH/PP Films

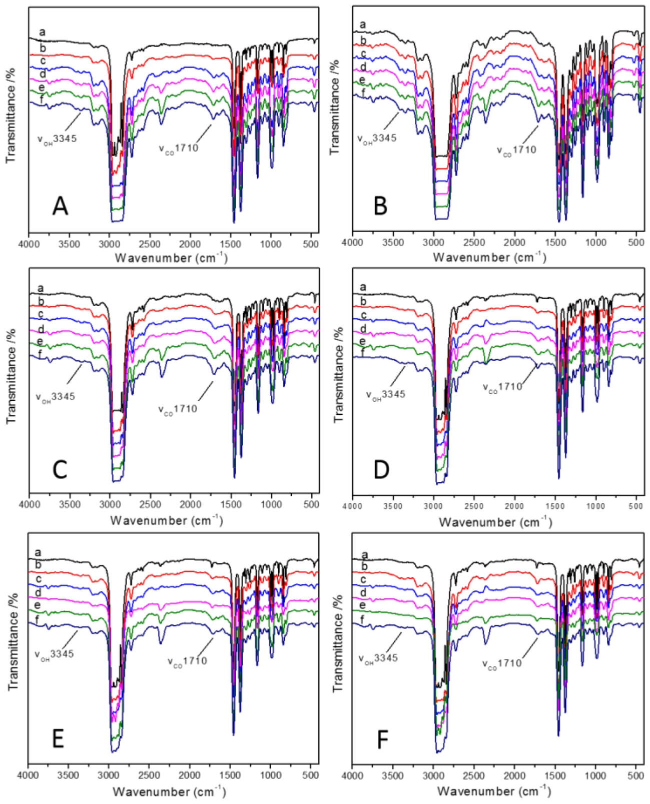

Figure 7. FT-IR spectra of (A) pristine PP, (B) ZnAl–NO_3-LDH/PP, (C) CPBA/PP, (D) 1 wt.% ZnAl–CPBA-LDH/PP, (E) 3 wt.% ZnAl–CPBA-LDH/PP and (F) 5 wt.% ZnAl–CPBA-LDH/PP after different UV exposure times (a, 0 min; b, 10 min; c, 20 min; d, 30 min; e, 40 min; f, 50 min).

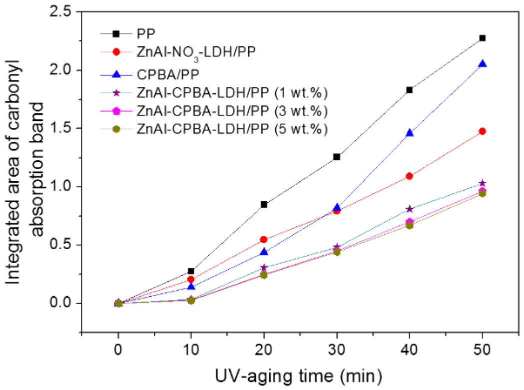

Figure 8. Integrated area of the carbonyl absorption band of pristine PP (squares), ZnAl–NO_3-LDH/PP (circles), CPBA/PP (triangles), 1 wt.% ZnAl–CPBA-LDH/PP (stars), 3 wt.% ZnAl–CPBA-LDH/PP (pentagon), and 5 wt.% ZnAl–CPBA-LDH/PP (hexagon) films as a function of exposure time.

To evaluate the efficacy of ZnAl–CPBA-LDH as a UV blocking agent for polymers, we added ZnAl–NO_3-LDH, CPBA and ZnAl–CPBA-LDH to separate samples of PP and carried out UV aging tests. The FT-IR spectra of pristine PP, ZnAl–NO_3-LDH/PP, CPBA/PP and ZnAl–CPBA-LDH/PP films after UV exposure are shown in Figure 8. The photooxidative and thermal degradation mechanism of PP has been widely studied.[11c, 20] The decomposition product shows two characteristic absorption peaks associated with carbonyl and hydroperoxide groups at 1710 and 3345 cm^{-1}, respectively. With increasing exposure time to UV light, the absorption intensities of PP at 1710 and 3345 cm^{-1} show a gradual increase. The aging degree of the PP can be quantified by calculating the area of the carbonyl absorption band in the region from 1810 to 1660 cm^{-1}, as shown in Figure 9.[21] The integrated area of the carbonyl absorption band of ZnAl–CPBA-LDH/PP increases more slowly with time than those for pristine PP, ZnAl–NO_3-LDH/PP and CPBA/PP, suggesting that ZnAl–CPBA-LDH can significantly inhibit the aging of PP. In particular, the area of the carbonyl absorption band for CPBA/PP increases significantly after irradiation for more than 30 min, indicating the poor photo- and thermal stability of the pristine CPBA. Therefore, the superior antiaging performance of ZnAl–CPBA-LDH compared with CPBA can be attributed to both the improvement in photo- and thermal stability of the organic guest by virtue of its interactions with the host layers, as well as the UV shielding properties of the inorganic layers. Additionally, the quantity optimization experiments showed that the adding amount of 3 wt.% of ZnAl–CPBA-LDH can achieve the highest photostability of PP, and the adding amount more than 5 wt.% of ZnAl–CPBA-LDH would influence the blending uniformity of PP/LDH composites.

Conclusion

A readily available fluorescent material CPB has been hydrolyzed into CPBA, and CPBA-intercalated LDH has been prepared by an ion-exchange method. Compared with the pristine CPBA, ZnAl–CPBA-LDH exhibits better UV blocking properties with longer fluorescence lifetime and higher photoluminescence quantum yield. Accelerated UV aging tests of PP samples containing CPBA and ZnAl–CPBA-LDH confirm the excellent UV blocking properties of the intercalated product, as shown by the significantly lower increase in the carbonyl band intensity during the aging of ZnAl–CPBA-LDH/PP when compared with pristine PP and CPBA/PP. Addition of only 3 wt.% ZnAl–CPBA-LDH affords excellent UV aging resistance, highlighting the potential practical applications of this material as an additive for PP, as well as other polymer materials which are also prone to UV aging. The UV blocking properties of the supramolecular ZnAl–CPBA-LDH host–guest material involve both shielding by the LDH layers and UV light absorption by the interlayer organic species. Furthermore, in contrast to conventional UV absorbing materials, the absorbed UV light is converted into visible fluorescence emission instead of thermal radiation, thus reducing thermal aging of the polymer materials.

Acknowledgments

This work was supported by the National Natural Science Foundation of China (NSFC), the National Basic Research Program of China (973 Program) (Grant No.2014CB932104), and Beijing Municipal Natural Science Foundation (Grant No. 2152016).

Notes and references

a: State Key Laboratory of Chemical Resource Engineering, Beijing University of Chemical Technology, Beijing 100029, P. R. China.
Fax: +86-10-64425385; Tel: +86-10-64412131;
E-mail: yandongpeng001@163.com (D. Yan);
linyj@mail.buct.edu.cn (Y. Lin)
b: Key Laboratory of Theoretical and Computational Photochemistry, Ministry of Education, College of Chemistry, Beijing Normal University, Beijing 100875, China, E-mail: yandp@bnu.edu.cn

1. (*a*) P. Bartolomeo, M. Irigoyen, E. Aragon, M. A. Frizzi and F. X. Perrin, *Polym. Degrad. Stabil.*, 2001, **72**, 63-68; (*b*) A. M. E. Sherbini, *World J. Nano Sci. Eng.*, 2012, **02**, 181-188.
2. (*a*) A. L. Andrady, H. Hamid and A. Torikai, *Photochem. Photobiol. Sci.*, 2011, **10**, 292-300; (*b*) R. P. Singh, N. S. Tomer and S. V. Bhadraiah, *Polym. Degrad. Stabil.*, 2001, **73**, 443-446.
3. (*a*) B. Gabrielle, C. Lorthioir and F. Laupretre, *J. Phys. Chem. B*, 2011, **115**, 12392-12400; (*b*) T. Poli, L. Toniolo and A. Sansonetti, *Macromol. Symp.*, 2006, **238**, 78-83.
4. (*a*) C. Decker, *Surf. Coat. Int. B. Coat. Trans.*, 2005, **88**, 9-17; (*b*) A. Salvador and A. Chisvert, *Anal. Chim. Acta.*, 2005, **537**, 1-14.
5. J. R. Castro Smirnov, M. E. Calvo and H. Miguez, *Adv. Funct. Mater.*, 2013, **23**, 2805-2811.
6. (*a*) P. Gago-Ferrero, M. Silvia Diaz-Cruz and D. Barcelo, *Anal. Bioanal. Chem.*, 2012, **404**, 2597-2610; (*b*) M. S. Diaz-Cruz, M. Llorca and D. Barcelo, *Trends Anal. Chem.*, 2008, **27**, 873-887.
7. (*a*) D. Yan, Y. Zhao, M. Wei, R. Liang, J. Lu, D. G. Evans and X Duan, *RSC Adv.*, 2013, **3**, 4303-4310; (*b*) G. Wang, D. Rao, K. Li and Y. Lin, *Ind. Eng. Chem. Res.*, 2014, **53**, 4165-4172; (*c*) D. Yan, S. Qin, L. Chen, J. Lu, J. Ma, M. Wei, D. G. Evans and X. Duan, *Chem. Commun.*, 2010, **46**, 8654-8656; (d) Y. Zhao, H. Lin, M. Chen and D. Yan, *Ind. Eng. Chem. Res.*, 2014, **53**, 3140–3147.
8. (*a*) M. Shao, J. Han, M. Wei, D. G. Evans and X. Duan, *Chem. Eng. J.*, 2011, **168**, 519-524; (*b*) L. Tian, Y. Zhao, S. He, M. Wei and X. Duan, *Chem. Eng. J.*, 2012, **184**, 261-267.
9. (*a*) J. Zhao, J. Chen, S. Xu, M. Shao, D. Yan, M. Wei, D. G. Evans and X. Duan, *J. Mater. Chem. A*, 2013, **1**, 8836; (*b*) J. Zhao, Z. Lu, M. Shao, D. Yan, M. Wei, D. G. Evans and X. Duan, *RSC. Adv.*, 2013, **3**, 1045.
10. C. Nyambo and C. A. Wilkie, *Polym. Degrad. Stabil.*, 2009, **94**, 506-512.
11. Y. Huang, Z. Feng, H. Zhang and J. Yu, *J. Test. Eval.*, 2012, 40, 734-739.
12. (*a*) Y. Dou, S. Xu, X. Liu, J. Han, H. Yan, M. Wei, D. G. Evans and X. Duan, *Adv. Funct. Mater.*, 2014, **24**, 514-521; (*b*) Y. Dou, A. Zhou, T. Pan, J. Han, M. Wei, D. G. Evans and X. Duan, *Chem. Commun.*, 2014, **50**, 7136.
13. S. B. Khan, C. Z. Liu, E. S. Jang, K. Akhtar and H. Han, *Mater. Lett.*, 2011, **65**, 2923-2926.
14. (*a*) Y. Zhao, F. Li, R. Zhang, D. G. Evans and X. Duan, *Chem. Mater.*, 2002, **14**, 4286-4291; (*b*) D. G. Evans and X. Duan, *Chem. Commun.*, **2006**, 485.
15. G. J. Cui, D. G. Evans and D. Q. Li, *Polym. Degrad. Stabil.*, 2010, **95**, 2082-2087.

16. D. Q. Li, Z. J. Tuo, D. G. Evans and X. Duan, *J. Solid. State. Chem.*, 2006, **179**, 3114-3120.
17. Z. P. Xu and H. C. Zeng, *Chem. Mater.*, 2001, **13**, 4564-4572.
18. D. Yan, J. Lu, M. Wei, D. G. Evans and X. Duan, *J. Mater. Chem.*, 2011, **21**, 13128.
19. (*a*) D. Yan, J. Lu, M. Wei, D. G. Evans and X. Duan, *Chem. Eng. J.*, 2013, **225**, 216-222; (*b*) D. Yan, J. Lu, L. Chen, S. Qin, J. Ma, M. Wei, D. G. Evans and X. Duan, *Chem. Commun.*, 2010, **46**, 5912-5914; (c) Y. Zhang, M. Song, R. Yun, Q. Meng and D. Yan, *Chin. J. Chem.*, 2014, **9**, 859-864.
20. (*a*) S. K. Sharma and S. K. Nayak, *Polym. Degrad. Stabil.*, 2009, **94**, 132-138; (*b*) P. He, Y. Xiao, P. Zhang, C. Xing, N. Zhu, X. Zhu and D. Yan, *Polym. Degrad. Stabil.*, 2005, **88**, 473-479.
21. Y. Feng, Y. Jiang, Q. Huang, S. Chen, F. Zhang, P. Tang and D. Li, *Ind. Eng. Chem. Res.*, 2014, **53**, 2287-2292.